Concurrent assessment of motor unit firing properties and fascicle length changes with high-density surface electromyography ultrasound-transparent electrodes

Eduardo Martinez-Valdes[1], *Francesco Negro[2], Alberto Botter[3,4], Giacinto Luigi Cerone[3,4], Deborah Falla[1], *Patricio A Pincheira[4], Glen A Lichtwark[5], Andrew G Cresswell[5]

[1] Centre of Precision Rehabilitation for Spinal Pain, School of Sport, Exercise and Rehabilitation Sciences, University of Birmingham, United Kingdom.

[2] Department of Clinical and Experimental Sciences, Universita` degli Studi di Brescia, Brescia, Italy.

[3] Laboratory for Engineering of the Neuromuscular System (LISiN), Department of Electronics and Telecommunication, Politecnico di Torino, Torino, Italy.

[4] PoliToBIOMed Lab, Politecnico di Torino, Turin, Italy.

[5]School of Human Movement and Nutrition Sciences, The University of Queensland, Australia

*Authors contributed equally

Corresponding Author:

Eduardo Martinez-Valdes

Centre of Precision Rehabilitation for Spinal Pain, School of Sport, Exercise and Rehabilitation Sciences, University of Birmingham, United Kingdom.

Edgbaston B15 2TT

e.a.martinezvaldes@bham.ac.uk

+44 0 121 4158187

Acknowledgments: This study was partially funded with the University of Birmingham International Engagement Fund (BIEF) awarded to EM-V.

ABSTRACT

Previous studies assessing relationships between muscle mechanics and neural activity have concurrently assessed changes in fascicle length (FL) and neural activation with electromyography (EMG) approaches with low spatial sampling from different muscle regions. This project aimed to assess changes in FL and motor unit (MU) firing, simultaneously, on the same region of interest, with high-density EMG electrodes transparent to ultrasound (HDEMG-US). EMG signals and ultrasound images were recorded simultaneously from the tibialis anterior of 10 participants, using a silicon matrix of 32 electrodes, while performing sustained-isometric ankle-dorsiflexion contractions, at diverse joint positions (0˚ and 30˚ plantar flexion) and torques (20% and 40% of maximum). EMG signals were decomposed into individual MUs and changes in FL were assessed with a fascicle-tracking algorithm. MU firing data was converted into a cumulative spike train (CST) that was cross-correlated with dorsiflexion torque (CST-torque) and FL (CST-FL). On average, 7 (3) MUs were identified across contractions. Cross-correlations showed that CST could explain on average 60% (range: 31-85%) and 71% (range: 0.31-0.88) of the variance in FL and torque, respectively. Cross-correlation lags revealed that the delay between CST-FL (~75ms) was smaller than CST-torque (~150ms, $p<0.001$). Finally, we could observe that both delays increased by ~20ms at 30° of plantar flexion ($p<0.05$). This study is the first to demonstrate the feasibility of recording single MU activity with HDEMG-US whilst simultaneously evaluating changes in FL. The findings show a close relationship between dorsiflexion torque, FL and CST, also allowing quantification of the delay between each of these signals.

INTRODUCTION

One of the most fundamental issues in motor control is to understand how the nervous system interacts with muscles for the generation and control of movement. While, some answers have been obtained from separate studies in the fields of neurophysiology and biomechanics, there has been a failure to effectively integrate these two disciplines in order to provide clearer information on how neural activity is influenced by muscle mechanics and vice-versa (Enoka, 2004; Tytell *et al.*, 2011). The integration of electromyography (EMG) recordings and ultrasound imaging has given important information about both the mechanisms of muscle activation and contraction, respectively (Hodges *et al.*, 2003; Brown & McGill, 2010; Barber *et al.*, 2013; Day *et al.*, 2013; Pincheira *et al.*, 2018). However, previous studies that have integrated these techniques have 1) utilized methods with low spatial resolution, 2) recorded ultrasound images and EMG signals from different muscle regions and 3) commonly have not employed motor unit recordings to directly assess the neural drive received by muscles. With respect to the first point, studies have employed amplitude estimates from bipolar surface EMG recordings in order to assess changes in neural activity and the resultant force produced by muscles (Suzuki *et al.*, 2021). Due to many factors such as crosstalk, amplitude cancellation and underlying changes in muscle length and velocity, surface EMG amplitude is unfortunately poorly correlated with the resultant force produced by muscles and therefore cannot be used to directly understand the neural determinants of muscle contractions (Negro *et al.*, 2009; Dideriksen *et al.*, 2018; Dideriksen & Farina, 2019). Regarding the second point, it has been shown that a muscle's activity is not homogeneous (Vieira & Botter, 2021), and therefore, i.e., changes in muscle architecture and/or morphology from different regions could potentially provide results that are

not related from those studied on the region of interest, which poses a problem when the ultrasound probe and EMG electrodes are positioned in different sections of the muscle. Regarding the final point, motor unit recordings provide a more thorough understanding of neuromechanical determinants of movement since motor units are responsible for transforming synaptic activity into muscle contractions. However, a relatively large sample is required to be able to correlate both the neural drive received by muscles and the forces produced at the muscle or tendon, an issue which is particularly difficult with classic intramuscular recordings (Farina *et al.*, 2016).

Ultrasound translucent high-density EMG (HDEMG-US) electrodes have been developed to tackle these issues (Botter *et al.*, 2013). Such setup allows simultaneous recording of high-density EMG with ultrasound images sampled from the same region of interest. This technique has the potential to improve our understanding of the neuromechanical determinants of movement, however to-date this method has not been used to relate single motor unit discharge characteristics (e.g. blind-source separation decomposition) with dynamic fascicle movement tracked from the ultrasound images.

Our primary aim was to develop a framework to assess motor unit firing characteristics in relation to muscle fascicle dynamics during force development and sustained isometric contraction. To demonstrate the efficacy of using fascicle length changes to understand modulations in motor unit discharge properties, we examined the relationship between motor unit cumulative spike train (CST) and both fascicle length changes and dorsiflexion torque output of the tibialis anterior muscle. Because the fascicle shortening during isometric contraction is related to force output (due to stretch of the in-series tendon), we expect the correlation between CST and fascicle

shortening will be similar to that between CST and torque, but with a reduced lag due to the faster conversion of motor unit activity into contraction (compared to the conversion of motor unit activity into torque). We also examined differences in recruitment threshold when considered in terms of fascicle length or torque, as possible delays between these signals, might affect the interpretation of motor unit recruitment and de-recruitment thresholds.

METHODS

The study was conducted at the school of Human Movement and Nutrition Sciences of the University of Queensland, Australia. All procedures were approved by the University of Queensland ethical committee (approval number: 2019001675) and were conducted in accordance with the Declaration of Helsinki. Ten healthy young male volunteers participated in the experiments [age: mean (SD) 29 (5) years]. Exclusion criteria included any neuromuscular disorder, musculoskeletal injuries such as muscle strain as well as any current or previous history of lower limb pain/injury and age <18 or >35 years. Participants were asked to avoid any strenuous activity 24 h before the measurements.

Task

Participants were seated in a reclined position on the chair of an isokinetic dynamometer (Humac Norm, CSMi Computer Sports Medicine, Stoughton, USA). The right leg (dominant for all participants) was extended and positioned over a support with the knee flexed to 10° (with 0° representing full knee extension). The centre of rotation of the ankle joint (lateral malleoli) was aligned to the centre of rotation of the isokinetic dynamometer in order to accurately quantify ankle dorsi-flexion torque. Participants performed sustained isometric dorsiflexion contractions

at varying torques at short (ankle at 0° plantar flexion) and long muscle lengths (ankle at 30° plantar flexion). A study schematic describing the measurements performed during the session can be seen on **Figure 1**. The session began with the participants' performing three isometric ankle dorsiflexion maximum voluntary contractions (MVC) at each ankle angle, where each MVC was separated by 2-min of rest. The order in which the ankle was positioned (short and long tibialis anterior lengths) was randomized. Following the MVC assessment, participants were allowed to practice with visual feedback of their exerted torque (displayed on a computer monitor), by performing brief ramp-hold contractions at low torque levels (20% MVC). Then, after 5 min of rest, participants performed ramp-hold contractions at 20% or 40% MVC. Participants were asked to increase their torque at a rate of 10% MVC/s and then to hold the contraction at the target level for 30 s, therefore reaching the 20% MVC target in 2 s and the 40% MVC in 4 s. Two sustained 20% MVC and two sustained 40% MVC contractions were performed.

Electromyography

Surface electromyography (EMG) signals were recorded from the tibialis anterior muscle using a high-density, 32-channel, HDEMG-US electrode grid (LiSIN, Torino, Italy) (Botter *et al.*, 2013). Each grid consists of 8 x 4 electrodes (1-mm diameter, 10-mm interelectrode distance in both directions) embedded into a layer of silicon rubber **Figure 2A**. The array was located centrally between the proximal and distal tendons of the muscle, with the columns oriented parallel to the tibia bone (Martinez-Valdes *et al.*, 2020b). Skin-electrode contact was made by inserting conductive gel (Sonogel, Bad Camberg, Germany) into the electrode cavities with a mechanical pipette (Eppendorf, Hamburg, Germany) as seen previously (Botter *et al.*, 2013). Signals were amplified and recorded using a new wireless wearable HDEMG amplifier (Cerone *et al.*, 2019)

(**Figure 2B),** directly connected to the grid of electrodes, which is ideal when HDEMG measurements are combined with other methods such as ultrasound imaging. The amplifier was light and compact (16.7 g and 3.4 cm x 3 cm x 1.5 cm), and contained a 16-bit analogue-digital converter. For this experiment, data was recorded in monopolar mode at a sampling frequency of 2048 Hz, with a gain of 192 ± 1 V/V and a band-pass filter with cut-off frequencies between 10-500 Hz. Torque data was also sampled at 2048Hz and recorded through the auxiliary input of the HDEMG amplifier. All EMG and torque data were processed and analysed offline using MATLAB 2019b (MathWorks Inc., Natick, MA).

Ultrasonography

Ultrasound images of tibialis anterior fascicles were captured using B-mode ultrasonography (6 MHz, ~80 frames per second, 60 mm field of view) using a 128-element multi-frequency transducer (LF9-5N60-A3; Telemed, Vilnius, Lithuania) attached to a PC-based ultrasound system (ArtUs EXT-1H scanner; Telemed, Vilnius, Lithuania). A dry HDEMG-US grid (without conductive gel) was first used to find the best alignment of the probe allowing clear visualization of the muscle's fascicles when the probe is placed over the electrodes. Once the optimal position was identified, the skin was marked with an indelible pen. Then, the HDEMG-US electrode grid electrode cavities were filled with conductive gel and positioned over the tibialis anterior muscle. The flat-shaped ultrasound transducer was then placed over the electrode grid and firmly strapped over the leg using an elastic bandage to prevent any movement. An example of the setup and an ultrasound image can be seen in **Figure 2B.**

HDEMG and ultrasound synchronization

Torque, position, HDEMG, and ultrasound data were synchronized utilising an analogue pulse sent from an AD board (Micro 1401-3, Cambridge Electronic Design, Cambridge, UK). The trigger signal was set at 80 Hz and controlled frame by frame the ultrasound recording (i.e. every time the beamformer received a pulse, one frame of ultrasound data was recorded). The same trigger signal was sent to the auxiliary input of the HDEMG device and was aligned offline with the tracked fascicle data (see next section) obtained from the ultrasound files.

Motor unit decomposition and fascicle length tracking

The HDEMG signals were decomposed into motor unit spike trains with an extensively validated blind source separation algorithm, which provides automatic identification of the activity of multiple single motor units (Negro *et al.*, 2016). Each identified motor unit was assessed for decomposition accuracy with a validated metric (Silhouette, SIL), which represents the sensitivity of the decomposed spike train. Since the identification of motor unit activity with HDEMG-US grids is more challenging due to the lower selectivity of these grids (i.e., 32 channels and inter-electrode distance of 10 mm), an accuracy level of 0.86 SIL (86% of accuracy) was used to approve or discard any motor unit (usual threshold is set at 0.90 SIL (Negro *et al.*, 2016; Martinez-Valdes *et al.*, 2020a). Moreover, further examination of each spike train was performed, and all firings separated from the next by <33.3 ms or >200 ms were re-checked manually by an experienced operator (Afsharipour *et al.*, 2020; Cogliati *et al.*, 2020). After this procedure, the averaged SIL value increased to 0.90 (0.007).

Tibialis anterior fascicle length changes were tracked offline by employing custom-made software (Farris & Lichtwark, 2016) utilizing a previously validated Lucas-Kanade optical flow algorithm with affine transformation (Gillett *et al.*, 2013; Farris & Lichtwark, 2016). From each

trial, we selected the fascicle in which we were able to visualize ~80% of its length within the field of view. We selected a fascicle from the anterior compartment of the tibialis anterior muscle because 1) this was the region of motor unit activity that was likely covered by the HDEMG electrode and 2) our preliminary results showed that changes in fascicle length from this region are enough to explain at least 70% of the variance in the resultant torque output (see results). Changes in fascicle length were analysed according to shortening length [Δ fascicle length (i.e. difference in fascicle length from rest to target torque (20% MVC)], in order to 1) understand the amount of fascicle shortening required to recruit a motor unit and reach the required torque level (20% MVC and 40% MVC), and 2) to be able to correlate fluctuations in fascicle length with fluctuations in motor unit discharge rate, since absolute changes in fascicle length go in an opposite direction to discharge rate (fascicle length decreases when discharge rate increases, see next section). We also estimated pennation angle as the angle between the fascicle and its insertion into the central aponeurosis (Reeves & Narici, 2003). The pennation angle was calculated when the muscle was at rest and when the torque was stable during the isometric contractions.

Concurrent motor unit and fascicle length analysis

For sustained isometric contractions, mean discharge rate was calculated from the stable plateau torque region. Motor unit recruitment and de-recruitment thresholds were defined as the ankle dorsiflexion torques (%MVC) or fascicle shortening lengths (Δfascicle length, mm) at the times when the motor units began and stopped discharging action potentials, respectively. For these contractions we also tested the possibility to track the same motor units across the two different target torques and muscle lengths, with a previously proposed method based on cross-

correlation of 2D MUAPs (Martinez-Valdes *et al.*, 2017b). In this procedure, MUAP matches between the two correlated trials (i.e. 20% MVC-0˚ vs 20% MVC-30˚) were visually inspected and the two identified motor units were regarded as the same when they had a cross-correlation coefficient >0.80 (Martinez-Valdes *et al.*, 2017b). Cross-correlation (time domain) analysis was also used to assess the interplay between torque, fascicle length and motor unit firing data. For this purpose, motor unit discharge times were summed to generate a cumulative spike train (CST) as done previously (Thompson *et al.*, 2018). Fascicle length signals (which were sampled at 80Hz) were interpolated to 2048Hz to match both motor unit and torque data. After these procedures, the CST, fascicle length and torque signals were low-pass filtered (4th order zero-phase Butterworth, 2Hz) and then high-pass filtered (4th order zero-phase Butterworth, 0.75Hz) as presented previously (De Luca & Erim, 1994). These filtered signals were then cross-correlated to assess similarities in their fluctuations (cross-correlation coefficient) and calculate the lags between CST vs torque, CST vs fascicle length and fascicle length vs torque. These assessments provided information on the delays generated between the neural drive and torque output, neural drive and muscle contraction and, muscle contraction and torque output.

Statistical Analysis

Results are expressed as mean and (SD). Normality of the data was assessed with the Shapiro-Wilk test and Sphericity was tested with the Mauchly test. Differences between fascicle parameters (Absolute changes in length and pennation angle) at short and long muscle lengths during rest were assessed with paired t-tests. Absolute differences in fascicle length and pennation angle during isometric contractions were assessed with a two-way repeated measures ANOVA, with factors of muscle length (0˚ or 30˚ of plantar flexion) and torque (20 or 40% MVC).

For motor unit/Δfascicle length data during isometric contractions the following statistical tests were employed: 1) two-way repeated measures ANOVA with factors of muscle length and torque to assess differences in discharge rate 2) three-way repeated measures ANOVA with factors of muscle length, torque and signal comparison (CST vs torque, fascicle length vs CST, and torque vs fascicle length) to assess differences in cross-correlation results (correlation coefficient and lag) 3) three-way repeated measures ANOVA with factors of muscle length, torque and recruitment (recruitment vs de-recruitment) to assess differences between recruitment and de-recruitment thresholds [in terms of %MVC torque and Δfascicle length]. All ANOVA analyses were followed by pairwise comparisons with a Student-Newman-Keuls (SNK) post hoc test when ANOVA was significant. Statistical significance was set at $p<0.05$.

RESULTS

Maximal torque, motor unit decomposition and tracking during isometric contractions

The MVC dorsiflexion torque differed at the two ankle positions and was 25.2 (13.2) and 51.8 (12.5) Nm at short (0° plantarflexion) and long (30° plantarflexion) muscle lengths, respectively ($P<0.001$). During the isometric contractions, an average of 7 (3), 7 (2), 7 (3) and 6 (2) motor units could be identified per participant at 20% MVC-0˚, 20% MVC-30˚, 40% MVC-5˚ and 40% MVC-30˚, respectively. A representative example with the decomposition results from one participant can be seen in **Figure 3.** In this particular example, each motor unit has a clearly distinct MUAP shape (right side of the figure) which allowed accurate identification of discharge times (left side of the figure). An average of 3 (2) motor units could be tracked successfully per participant across the two muscle lengths [2D MUAP cross-correlation coefficient 0.83 (0.03)] and 3 (1) motor units per participant across the two torque levels [2D MUAP cross-correlation coefficient 0.88 (0.05)]. A

247 representative example of the tracking procedure across the two joint angles with the HDEMG-
248 US grids can be seen in **Figure 4**.

249 *Relationships between fascicle length, torque and motor unit discharge rate during isometric*
250 *contractions*

251 Absolute fascicle lengths and pennation angles during rest and isometric contractions at the
252 different torque targets and joint angles are presented in **Table 1.** Overall, tibialis anterior
253 fascicles were longer and had smaller pennation angles at 30˚ of plantar flexion at rest and during
254 contractions ($p<0.001$). Nevertheless, fascicle lengths decreased (torque effect: $p<0.001$,
255 $\eta^2=0.78$) and pennation angles increased (torque effect: $p=0.018$, $\eta^2=0.48$) similarly with
256 increasing torque at both 0˚ and 30˚ of plantarflexion.

257

Table 1. Fascicle length and pennation angles at rest and during isometric contractions at 20% and 40% MVC in short and long muscle lengths

	Short (0˚plantar flexion)	**Long (30˚ plantar flexion)**	**P-value**
Pennation angle (°), rest	15.2 (1.7)	12.0 (1.7)	<0.001
Fascicle length (mm), rest	60.2 (8.8)	74.5 (9.1)	<0.001
Pennation angle (°), 20% MVC	19.2 (3.7)	16.9 (3.9)	0.001#
Fascicle length (mm), 20% MVC	52.7 (7.5)	66.3 (9.4)	<0.001*
Pennation angle (°), 40% MVC	20.8 (3.1)	17.4 (4.0)	0.001#
Fascicle length (mm), 40% MVC	50.8 (6.9)	61.9 (7.9)	<0.001*

*Significant effect of torque ($p<0.001$)
#Significant effect of torque ($p=0.018$)

258 Similar to the changes in fascicle length, the tracking of individual motor units across short and
259 long muscle lengths revealed similar discharge rates at the different joint angles (15.3 (2.6) Hz
260 and 14.7 (1.4) Hz at 20% MVC in 0˚ of plantar flexion, and 16.7 (2.3) Hz and 17.0 (2.4) Hz at 40%

MVC in 30˚ of plantar flexion, muscle length effect: P=0.74, η2=0.047), but increased firing frequency between the different torque levels (torque effect: P=0.03, η^2=0.43). A representative example of the concurrent assessment of changes in fascicle length, torque and CST can be seen in **Figure 5.** Briefly, after the offline identification/tracking of the fascicle (**Figure 5A**), and the identification/editing of the motor unit spike trains and subsequent conversion to CSTs, three signals were obtained: torque, fascicle length and CST. All these signals were then cross-correlated on the stable torque part of the contraction (**Figure 5B**, upper panel) in order to assess common fluctuations between torque, CST and fascicle length signals. All comparisons showed high levels of cross-correlation (CST vs torque, CST vs fascicle length and fascicle vs torque) and the lags obtained, showed the delay between: neural drive and resultant torque output (CST vs torque), neural drive and muscle contraction (CST vs fascicle length) and, muscle contraction and resultant torque output (fascicle length vs torque). The cross-correlation results for the group of participants are presented in **Table 2**. Overall, all cross-correlation coefficients were high as each of the signals could explain on average, at least 50% of the variance in resultant torque, CST and fascicle length, showing that there was a strong relationship between these variables. Nevertheless, the cross-correlation between CST vs fascicle length was significantly smaller compared to the other signal comparisons (signal comparison effect: P=0.007, η2=0.427). Cross-correlation lags (**Figure 6**) during sustained isometric contractions at 30˚ of plantar flexion were larger than those at 0˚ plantar flexion at both torque levels in all signal comparisons (muscle length effect: P=0.002, η2=0.66).

Table 2. Cross-correlation coefficients for comparisons between cumulative spike train (CST) vs torque, CST vs fascicle length and torque vs fascicle length during isometric contractions.

	Short length 20% MVC	**Long Length 20% MVC**	**Short length 40%MVC**	**Long length 40% MVC**
Steady isometric contractions				
Torque vs CST	0.74 (0.65-0.88)	0.74 (0.62-0.85)	0.74 (0.63-0.85)	0.61 (0.31-0.78)
Fascicle vs CST	0.64 (0.51-0.81)	0.57 (0.31-0.75)	0.63 (0.33-0.85)	0.50 (0.31-0.66)
Torque vs Fascicle	0.71 (0.40-0.88)	0.67 (0.33-0.89)	0.78 (0.33-0.93)	0.72 (0.50-0.91)

Results are expressed as mean (min-max range).

Variations in fascicle length and recruitment threshold and during isometric contractions

Motor unit recruitment and de-recruitment thresholds in terms of both Δfascicle length (mm) and torque (%MVC) are shown for a representative participant in **Figure 7A**. The figure shows that recruitment threshold torque is higher than the torque at de-recruitment, however, the Δfascicle length at which motor units were recruited and de-recruited was similar. This was confirmed in motor units that were tracked across short and long muscle lengths as de-recruitment thresholds were consistently lower when assessed in terms of %MVC torque (recruitment-de-recruitment effect: $P=0.029$, $\eta^2=0.43$, **Figure 7B**) but similar in terms of Δfascicle length (recruitment-de-recruitment effect $P=0.805$, $\eta^2=0.007$, **Figure 7B**,). In addition, although recruitment and de-recruitment thresholds increased in terms %MVC torque across 20% and 40% MVC levels (torque effect: $P=0.001$, $\eta^2=0.701$), motor units were recruited and de-recruited at a similar Δfascicle length with increasing torque (torque effect: $P=0.731$, $\eta^2=0.014$). Finally, recruitment-de-recruitment thresholds also increased at long muscle lengths (0° plantar flexion vs 30° plantar flexion) when considered as %MVC torque (muscle length effect: $P<0.001$, $\eta^2=0.77$) but not in terms of Δfascicle length (muscle length effect: $P=0.389$, $\eta^2=0.014$).

DISCUSSION

This is the first study showing simultaneous assessment of motor unit firing properties with changes in fascicle length, on the same region of interest, with HDEMG-US electrodes. Most importantly, these changes could be analysed at different torque levels and over a relatively large range of ankle joint motion (0˚ to 30˚ of plantar flexion). With the combination of these techniques, we identified strong relationships between fluctuations in tibialis anterior discharge rate and fascicle length, as well as fluctuations in fascicle length and the torque produced. These relationships allowed us to quantify the delays between motor unit firing activity and muscle contraction, and muscle contraction and joint torque. As we hypothesised, we were able to show that the delay between CST and fascicle length was smaller than that of CST and torque, which shows that previous measures of electromechanical delay between EMG (Cavanagh & Komi, 1979) or motor unit discharge patterns (Del Vecchio *et al.*, 2018) and force/torque might not provide an adequate estimation of the conversion neural activity into contraction. In addition, we could show that the delays between the neural drive and fascicle length or the generated force/torque are larger when the muscle contracts isometrically at longer fascicle lengths (**Figure 6**). Finally, due to the possibility to track motor units across different muscle lengths and target torques, we were also able to show that recruitment and de-recruitment thresholds are similar when considered in terms of fascicle length, meaning that motor units are recruited and de-recruited at the same relative fascicle length, regardless of the joint position or torque exerted. Taken together, the findings of the present study have enhanced our understanding of the interaction between motor unit firing and mechanisms of muscle contraction.

This study is the first to decompose motor unit activity from HDEMG-US grids. The findings showed that an average of 7 motor units could be accurately identified per participant during isometric contractions. The motor units identified with HDEMG-US electrodes had clear distinct MUAP shapes and show differences in activity across different regions of the electrode grid (**Figure 3**). Moreover, by employing the 2D spatial representation of MUAPs we were able to track approximately 40% of the identified motor units across torques and joint angles (**Figure 4**). We previously showed the possibility to track motor units across different force levels with HDEMG, by employing 2D MUAP "signatures" (Martinez-Valdes *et al.*, 2017b). Indeed, the advantage of HDEMG systems is that they show a large spatial representation of MUAPs, which can be used to follow the same units within and across sessions. This methodology has been successfully employed in a number of studies (Martinez-Valdes *et al.*, 2017a; Boccia *et al.*, 2019; Del Vecchio *et al.*, 2019; Murphy *et al.*, 2019). We expanded on that possibility and tracked motor units across different muscle lengths obtaining good results (average 83% of correlation between MUAPs). This shows that HDEMG-US electrodes allow the concurrent assessment of changes in motor unit discharge and fascicle length and linking those changes to motor units that can be followed across different joint angles and torque levels, enabling a more reliable assessment of neuromechanical variables. Nevertheless, it is important to mention that the number of channels of these new HDEMG-US grids was half of what has been used previously for the decomposition of HDEMG signals during voluntary contractions. For this reason, the number of identified motor units in the present study was lower than previous reports (see limitations).

A number of studies have shown that fluctuations in firing rate are closely related to the fluctuations in torque/force (Negro *et al.*, 2009; Del Vecchio *et al.*, 2018; Thompson *et al.*, 2018).

Considering this observation, we attempted to quantify the level of correlation between fluctuations in firing rate (CST), changes in fascicle length and torque, in order to first, corroborate that the information obtained from the identified motor units was linked to the fascicles of the region of interest (CST vs fascicle length correlation) and also to confirm that motor unit firings identified with HDEMG-US grids would be able to predict the torque produced via the tendon. The findings showed that all signals compared had high levels of correlation (CST explained ~70% (Negro *et al.*, 2009) and ~60% of the variance in torque and fascicle length respectively), confirming that the motor unit data obtained from HDEMG-US grids provided a good representation of the fascicle behaviour of the region of interest. The lower correlation between CST and fascicle length (**Table 2**) could be explained by a number of factors, including the subtle inaccuracies in fascicle length determination from ultrasound imaging and potential mismatches between fibres contributing to CST and the fibres in the imaging region. It is possible that the fascicle tracking code or the sampling frequency employed to obtain the images (80Hz) was not sensitive enough to detect smaller changes in fascicle length during sustained contractions. However, the sampling frequency is well above the frequency of variation in force during isometric contraction (<5Hz (Farina & Negro, 2015)) and tremor (5-13Hz, (Yavuz *et al.*, 2015)). Therefore, it is more likely that limitations in imaging the muscle in single plane and the resolution of the tracking algorithm may contribute to the lower correlations. The depth at which we tracked the fascicles (superficial portion of the tibialis anterior) vs region of motor units recorded may also contribute to discrepancies in the signal correlations. However, the HDEMG-US electrodes are most likely to only detect motor unit activity of the most superficial motor units (Farina *et al.*, 2002). If we also consider that blind-source separation motor unit decomposition

techniques favour the identification of motor units showing the largest MUAPs and the highest spatial localization on the HDEMG grid (Holobar & Farina, 2014; Negro *et al.*, 2016), it is very likely that the motor units included in the analysis mainly represent the superficial region of tibialis anterior. Nevertheless, it is important to note that our technique provided moderate-high cross-correlations between CST and fascicle length during isometric contractions, which demonstrates feasibility of using such approach to understand the link between motor unit recruitment and muscle mechanics during actual movement.

One of the most interesting findings from this study was the possibility of quantifying delays between CST vs. fascicle length and fascicle length vs. torque. Cross-correlation lags revealed that the time required to shorten the fascicle (conversion of motor unit firings into contraction) was smaller than the time required to produce mechanical output (torque). This finding implies that imaging of the muscle is necessary to determine the time required to convert motor unit discharge activity into contraction. Historically, the conversion of neural activity into mechanical output has been usually assessed by calculating the time-difference between the onset of force/torque and muscle activation (also known as the electromechanical delay (Cavanagh & Komi, 1979)). This assessment, however, assumes that there is no lag between the generation of a contraction and the transmission of force to the tendon. More recent studies that have combined conventional bipolar EMG and ultrasound during voluntary contractions have found that fascicle shortening happen before force/torque is generated (Begovic *et al.*, 2014; Ling *et al.*, 2020), which agrees with our findings. Nevertheless, this assessment has several issues, first, the onset of muscle activation from bipolar EMG signals can be greatly influenced by the electrode's location (Hug *et al.*, 2011), second, fascicle shortening from deeper muscle regions

could happen before EMG activity is detected on the surface (Dieterich *et al.*, 2017) and third, the assessment can be confounded by the mechanical impedances of the measuring device (Corcos *et al.*, 1992). Thus, absolute values of electromechanical delay might not provide a reliable assessment of the mechanisms responsible for force generation and transmission (Corcos *et al.*, 1992). For these reasons, we propose that cross-correlation of signals obtained from HDEMG-US motor unit decomposition and ultrasound could provide a better estimation of these delays, as such assessment considers mechanisms responsible for contraction dynamics (i.e. fascicle length responses to firing rate modulations) rather than just assessing delay differences between signals at contraction onset. Nevertheless, it is important to mention that our proposed approach shows longer delays in comparison with classical estimations of electromechanical delay (~150ms of delay between CST and torque vs. ~50ms between EMG and torque (Begovic *et al.*, 2014)), possibly due to the time-instant in which these relationships are quantified (contraction onset vs. sustained contraction), twitch characteristics of the active motor units (Del Vecchio *et al.*, 2018) and changes in MUAP duration during the contraction. Improved HDEMG decomposition techniques allowing accurate identification of motor unit activity before contraction onset (which is not currently possible), would allow comparing the delays obtained during force development and sustained contractions, in order to assess potential differences in signal transmission in different phases of isometric contractions.

Another interesting result obtained from the cross-correlation lags was that both CST vs. fascicle length and fascicle length vs. torque delays increased when the muscle contracted isometrically in a lengthened position (**Figure 6**). Changes in the duration of muscle-fibre twitch force and muscle-tendon compliance at larger muscle lengths likely influenced these delays. To provide

406 support to the first observation, several studies have reported that muscle twitches are
407 significantly larger (greater contraction and half-relaxation times) when the muscle is lengthened
408 (Stephens *et al.*, 1975; Marsh *et al.*, 1981; Bigland-Ritchie *et al.*, 1992). Therefore, it is very likely
409 that an increase in the overall duration of the motor unit responses at longer lengths is the reason
410 for the more delayed muscle contraction and transmission of force to the tendon observed at
411 the two submaximal normalized torque targets (20 and 40% MVC). In addition, changes in tendon
412 and aponeurosis elasticity during lengthening could also reduce the amount of neural drive
413 required to activate the muscle (Lichtwark & Wilson, 2007; Mayfield *et al.*, 2016; Raiteri *et al.*,
414 2018) and potentially increase the delays between signals. Nevertheless, the assessment of both
415 motor unit contractile properties and the effect of passive structural properties of the muscle on
416 motor unit behaviour needs to be confirmed in future investigations. The assessment of these
417 delays holds great potential in both healthy populations (i.e. aging) and patients (i.e. cerebral
418 palsy), as they could help to quantify impairments in force transmission, when muscles have
419 altered architecture (i.e. muscle contractures).
420 The current methodology presents multiple opportunities to assess interactions between motor
421 unit firing rate/recruitment and changes in fascicle length, however, for this methodological
422 report we wanted to focus on the assessment of recruitment and de-recruitment thresholds in
423 relation to both %MVC torque and fascicle length. We selected these variables because motor
424 unit studies typically use torque to assume changes in muscle behaviour, and delays between
425 motor unit firing and torque due to force transmission delays (along muscle/tendon and also
426 within dynamometer) would create offsets when comparing recruitment (torque rise) vs
427 decruitment (torque drop). The findings from this study in these assessed variables, emphasise

the need of quantifying changes in motor unit activity and fascicle length simultaneously. First, we were able to observe that recruitment and de-recruitment thresholds differed when quantified as % MVC torque (recruitment threshold was higher than the de-recruitment threshold) but were similar when quantified in terms of fascicle length. To our knowledge, this is the first study showing this discrepancy. Moreover, we were able to observe that the length at which a motor unit was recruited and de-recruited was maintained across joint angles and torque levels. Fascicle shortening preceded torque generation (as expected), but fascicles returned to resting values after the dorsiflexion torque returned to 0 Nm, meaning that during the ramp-down phase of the contraction, there is a time-point where the muscle returns passively to its original length (**Figure 7**). This can explain why most previous studies show lower torque values for de-recruitment than recruitment when considered as %MVC torque or absolute torque (De Luca, 1985; Romaiguere *et al.*, 1993) and emphasizes the need to quantify these thresholds in terms of fascicle length and not in terms of joint force/torque. Interestingly, similar divergences were recently reported when considering recruitment and de-recruitment in terms of joint angle or fascicle length during isometric plantarflexion contractions at varying knee-joint angles (Lauber *et al.*, 2014).

In this study we were able identify an average of 7 motor units across contractions, which is lower than the number of units identified with non-transparent HDEMG electrodes, where approximately 15 to 20 motor units can be identified on the tibialis anterior muscle on average per participant (Martinez-Valdes *et al.*, 2020b). These differences can be attributed to a number of factors. First, the grid of electrodes employed in the current study contained 32 electrodes vs. the 64 electrodes conventionally employed to decompose EMG signals. It has been shown that a

larger number of channels enhances the spatial identification of MUAPs and therefore improves the separation of the multiple motor unit sources from the HDEMG with blind-source separation methods (Farina *et al.*, 2008; Negro *et al.*, 2016). Second, the inter-electrode distance of the HDEMG-US grid (10mm) is less selective than the 64-channel grids (8mm) commonly employed to decompose motor unit activity, which can again influence the separation of MUAPs from the HDEMG. Therefore, improvements in electrode construction will likely increase the number of motor units identified with HDEMG-US. Nevertheless, it is important to mention that we were still able to explain ~70% of the of the variance in torque with the number of identified units in the present study, which is similar to the values reported in previous studies (Negro *et al.*, 2009; Del Vecchio *et al.*, 2018; Thompson *et al.*, 2018). Finally, and as mentioned previously, muscle fascicle imaging using ultrasound also has some limitations in terms of the resolution of the image and ability to track length changes, as well as the limitation of only being able to image one plane of the muscle. Improvements in ultrasound probe construction and/or the addition of another ultrasound probe in a different portion of the electrode grid would likely help to improve estimations of changes in fascicle length during isometric contractions.

In conclusion, this study presents, for the first time, the possibility to identify motor units and track changes in fascicle length simultaneously, on the same region of interest, with HDEMG-US electrodes. We showed that this method can be employed over a wide range of conditions, and can provide important information about the inter-relationships between neural drive, fascicle length and torque, which provides new opportunities to assess the neural and mechanical determinants of muscle contractions in both health and disease.

REFERENCES

Afsharipour B, Manzur N, Duchcherer J, Fenrich KF, Thompson CK, Negro F, Quinlan KA, Bennett DJ & Gorassini MA. (2020). Estimation of self-sustained activity produced by persistent inward currents using firing rate profiles of multiple motor units in humans. *J Neurophysiol* **124,** 63-85.

Barber LA, Barrett RS, Gillett JG, Cresswell AG & Lichtwark GA. (2013). Neuromechanical properties of the triceps surae in young and older adults. *Exp Gerontol* **48,** 1147-1155.

Begovic H, Zhou GQ, Li T, Wang Y & Zheng YP. (2014). Detection of the electromechanical delay and its components during voluntary isometric contraction of the quadriceps femoris muscle. *Front Physiol* **5,** 494.

Bigland-Ritchie BR, Furbush FH, Gandevia SC & Thomas CK. (1992). Voluntary discharge frequencies of human motoneurons at different muscle lengths. *Muscle Nerve* **15,** 130-137.

Boccia G, Martinez-Valdes E, Negro F, Rainoldi A & Falla D. (2019). Motor unit discharge rate and the estimated synaptic input to the vasti muscles is higher in open compared with closed kinetic chain exercise. *J Appl Physiol (1985)* **127,** 950-958.

Botter A, Vieira TM, Loram ID, Merletti R & Hodson-Tole EF. (2013). A novel system of electrodes transparent to ultrasound for simultaneous detection of myoelectric activity and B-mode ultrasound images of skeletal muscles. *J Appl Physiol (1985)* **115,** 1203-1214.

Brown SH & McGill SM. (2010). A comparison of ultrasound and electromyography measures of force and activation to examine the mechanics of abdominal wall contraction. *Clin Biomech (Bristol, Avon)* **25,** 115-123.

Cavanagh PR & Komi PV. (1979). Electromechanical delay in human skeletal muscle under concentric and eccentric contractions. *Eur J Appl Physiol Occup Physiol* **42,** 159-163.

Cerone GL, Botter A & Gazzoni M. (2019). A Modular, Smart, and Wearable System for High Density sEMG Detection. *IEEE Trans Biomed Eng* **66,** 3371-3380.

Cogliati M, Cudicio A, Martinez-Valdes E, Tarperi C, Schena F, Orizio C & Negro F. (2020). Half marathon induces changes in central control and peripheral properties of individual motor units in master athletes. *J Electromyogr Kinesiol* **55,** 102472.

Corcos DM, Gottlieb GL, Latash ML, Almeida GL & Agarwal GC. (1992). Electromechanical delay: An experimental artifact. *J Electromyogr Kinesiol* **2,** 59-68.

512 Day JT, Lichtwark GA & Cresswell AG. (2013). Tibialis anterior muscle fascicle dynamics adequately
513 represent postural sway during standing balance. *J Appl Physiol (1985)* **115,** 1742-1750.

514
515 De Luca CJ. (1985). Control properties of motor units. *J Exp Biol* **115,** 125-136.

516
517 De Luca CJ & Erim Z. (1994). Common drive of motor units in regulation of muscle force. *Trends Neurosci*
518 **17,** 299-305.

519
520 Del Vecchio A, Casolo A, Negro F, Scorcelletti M, Bazzucchi I, Enoka R, Felici F & Farina D. (2019). The
521 increase in muscle force after 4 weeks of strength training is mediated by adaptations in motor
522 unit recruitment and rate coding. *J Physiol* **597,** 1873-1887.

523
524 Del Vecchio A, Ubeda A, Sartori M, Azorin JM, Felici F & Farina D. (2018). Central nervous system
525 modulates the neuromechanical delay in a broad range for the control of muscle force. *J Appl*
526 *Physiol (1985)* **125,** 1404-1410.

527
528 Dideriksen JL & Farina D. (2019). Amplitude cancellation influences the association between frequency
529 components in the neural drive to muscle and the rectified EMG signal. *PLoS Comput Biol* **15,**
530 e1006985.

531
532 Dideriksen JL, Negro F, Falla D, Kristensen SR, Mrachacz-Kersting N & Farina D. (2018). Coherence of the
533 Surface EMG and Common Synaptic Input to Motor Neurons. *Front Hum Neurosci* **12,** 207.

534
535 Dieterich AV, Botter A, Vieira TM, Peolsson A, Petzke F, Davey P & Falla D. (2017). Spatial variation and
536 inconsistency between estimates of onset of muscle activation from EMG and ultrasound. *Sci Rep*
537 **7,** 42011.

538
539 Enoka RM. (2004). Biomechanics and neuroscience: a failure to communicate. *Exerc Sport Sci Rev* **32,** 1-3.

540
541 Farina D, Cescon C & Merletti R. (2002). Influence of anatomical, physical, and detection-system
542 parameters on surface EMG. *Biol Cybern* **86,** 445-456.

543
544 Farina D & Negro F. (2015). Common synaptic input to motor neurons, motor unit synchronization, and
545 force control. *Exerc Sport Sci Rev* **43,** 23-33.

546
547 Farina D, Negro F, Gazzoni M & Enoka RM. (2008). Detecting the unique representation of motor-unit
548 action potentials in the surface electromyogram. *J Neurophysiol* **100,** 1223-1233.

549
550 Farina D, Negro F, Muceli S & Enoka RM. (2016). Principles of Motor Unit Physiology Evolve With Advances
551 in Technology. *Physiology (Bethesda)* **31,** 83-94.

552
553 Farris DJ & Lichtwark GA. (2016). UltraTrack: Software for semi-automated tracking of muscle fascicles in
554 sequences of B-mode ultrasound images. *Comput Methods Programs Biomed* **128,** 111-118.

555
556 Gillett JG, Barrett RS & Lichtwark GA. (2013). Reliability and accuracy of an automated tracking algorithm
557 to measure controlled passive and active muscle fascicle length changes from ultrasound. *Comput*
558 *Methods Biomech Biomed Engin* **16,** 678-687.

559
560 Hodges PW, Pengel LH, Herbert RD & Gandevia SC. (2003). Measurement of muscle contraction with
561 ultrasound imaging. *Muscle Nerve* **27,** 682-692.

562
563 Holobar A & Farina D. (2014). Blind source identification from the multichannel surface electromyogram.
564 *Physiol Meas* **35,** R143-165.

565
566 Hug F, Lacourpaille L & Nordez A. (2011). Electromechanical delay measured during a voluntary
567 contraction should be interpreted with caution. *Muscle Nerve* **44,** 838-839.

568
569 Lauber B, Lichtwark GA & Cresswell AG. (2014). Reciprocal activation of gastrocnemius and soleus motor
570 units is associated with fascicle length change during knee flexion. *Physiol Rep* **2**.

571
572 Lichtwark GA & Wilson AM. (2007). Is Achilles tendon compliance optimised for maximum muscle
573 efficiency during locomotion? *J Biomech* **40,** 1768-1775.

574
575 Ling YT, Ma CZ, Shea QTK & Zheng YP. (2020). Sonomechanomyography (SMMG): Mapping of Skeletal
576 Muscle Motion Onset during Contraction Using Ultrafast Ultrasound Imaging and Multiple Motion
577 Sensors. *Sensors (Basel)* **20**.

578
579 Marsh E, Sale D, McComas AJ & Quinlan J. (1981). Influence of joint position on ankle dorsiflexion in
580 humans. *J Appl Physiol Respir Environ Exerc Physiol* **51,** 160-167.

581
582 Martinez-Valdes E, Falla D, Negro F, Mayer F & Farina D. (2017a). Differential Motor Unit Changes after
583 Endurance or High-Intensity Interval Training. *Med Sci Sports Exerc* **49,** 1126-1136.

584
585 Martinez-Valdes E, Negro F, Falla D, Dideriksen JL, Heckman CJ & Farina D. (2020a). Inability to increase
586 the neural drive to muscle is associated with task failure during submaximal contractions. *J*
587 *Neurophysiol* **124,** 1110-1121.

588
589 Martinez-Valdes E, Negro F, Farina D & Falla D. (2020b). Divergent response of low- versus high-threshold
590 motor units to experimental muscle pain. *J Physiol* **598,** 2093-2108.

591

592 Martinez-Valdes E, Negro F, Laine CM, Falla D, Mayer F & Farina D. (2017b). Tracking motor units
593 longitudinally across experimental sessions with high-density surface electromyography. *J Physiol*
594 **595,** 1479-1496.

595
596 Mayfield DL, Cresswell AG & Lichtwark GA. (2016). Effects of series elastic compliance on muscle force
597 summation and the rate of force rise. *J Exp Biol* **219,** 3261-3270.

598
599 Murphy S, Durand M, Negro F, Farina D, Hunter S, Schmit B, Gutterman D & Hyngstrom A. (2019). The
600 Relationship Between Blood Flow and Motor Unit Firing Rates in Response to Fatiguing Exercise
601 Post-stroke. *Front Physiol* **10,** 545.

602
603 Negro F, Holobar A & Farina D. (2009). Fluctuations in isometric muscle force can be described by one
604 linear projection of low-frequency components of motor unit discharge rates. *J Physiol* **587,** 5925-
605 5938.

606
607 Negro F, Muceli S, Castronovo AM, Holobar A & Farina D. (2016). Multi-channel intramuscular and surface
608 EMG decomposition by convolutive blind source separation. *J Neural Eng* **13,** 026027.

609
610 Pincheira PA, Hoffman BW, Cresswell AG, Carroll TJ, Brown NAT & Lichtwark GA. (2018). The repeated
611 bout effect can occur without mechanical and neuromuscular changes after a bout of eccentric
612 exercise. *Scand J Med Sci Sports* **28,** 2123-2134.

613
614 Raiteri BJ, Cresswell AG & Lichtwark GA. (2018). Muscle-tendon length and force affect human tibialis
615 anterior central aponeurosis stiffness in vivo. *Proc Natl Acad Sci U S A* **115,** E3097-E3105.

616
617 Reeves ND & Narici MV. (2003). Behavior of human muscle fascicles during shortening and lengthening
618 contractions in vivo. *J Appl Physiol (1985)* **95,** 1090-1096.

619
620 Romaiguere P, Vedel JP & Pagni S. (1993). Comparison of fluctuations of motor unit recruitment and de-
621 recruitment thresholds in man. *Exp Brain Res* **95,** 517-522.

622
623 Stephens JA, Reinking RM & Stuart DG. (1975). The motor units of cat medial gastrocnemius: electrical
624 and mechanical properties as a function of muscle length. *J Morphol* **146,** 495-512.

625
626 Suzuki R, Kanehisa H, Washino S, Watanabe H, Shinohara M & Yoshitake Y. (2021). Reconstruction of net
627 force fluctuations from surface EMGs of multiple muscles in steady isometric plantarflexion. *Exp*
628 *Brain Res* **239,** 601-612.

629
630 Thompson CK, Negro F, Johnson MD, Holmes MR, McPherson LM, Powers RK, Farina D & Heckman CJ.
631 (2018). Robust and accurate decoding of motoneuron behaviour and prediction of the resulting
632 force output. *J Physiol* **596,** 2643-2659.

Tytell ED, Holmes P & Cohen AH. (2011). Spikes alone do not behavior make: why neuroscience needs biomechanics. *Curr Opin Neurobiol* **21,** 816-822.

Vieira TM & Botter A. (2021). The Accurate Assessment of Muscle Excitation Requires the Detection of Multiple Surface Electromyograms. *Exerc Sport Sci Rev* **49,** 23-34.

Yavuz US, Negro F, Falla D & Farina D. (2015). Experimental muscle pain increases variability of neural drive to muscle and decreases motor unit coherence in tremor frequency band. *J Neurophysiol* **114,** 1041-1047.

660 **FIGURE LEGENDS**

661 **Figure 1.** Study schematic. MVC, maximum voluntary contraction torque.

662 **Figure 2.** High-density surface electromyography (HDEMG) ultrasound-transparent electrodes.
663 A) Back (up) and front (down) of the 32-channel (10 mm inter-electrode distance) electrode grid.
664 B) HDEMG electrode grid with 32-channel HDEMG amplifier (connected on top of the electrode)
665 and flat ultrasound probe can be seen on the left. Ultrasound image of proximal tibialis anterior
666 muscle can be seen on the right. Note the quality of the image with accurate visualization of
667 fascicles and, superficial, intermediate and deep aponeuroses.

668 **Figure 3.** Motor unit identification during isometric contractions. A total of 11 motor units (MUs)
669 were decomposed from the HDEMG signals in a representative participant during an isometric
670 contraction at 20% of the maximum voluntary torque (0° of plantarflexion). Instantaneous firing
671 rate with torque profile can be seen on the left of the figure while 2D motor unit action potentials
672 (MUAPs) from each of these motor units can be seen on the right of the figure. Note the clear
673 differences in MUAP shape for each of the identified units.

674 **Figure 4.** Motor unit tracking. A representative example of a motor unit that was tracked across
675 two-plantarflexion angles at 20% MVC can be seen on the figure. For this motor unit, the action
676 potentials (top of the figure) had a cross correlation coefficient of 0.91 across angles. The
677 instantaneous firing rate of this unit can be seen on the bottom of the figure.

678 **Figure 5.** Fascicle length tracking procedure and correlation with torque and motor unit data. A)
679 A tibialis anterior ultrasound image and a fascicle of interest (red) can be seen on top of the
680 figure. The length data obtained from the tracking of this fascicle was then correlated with torque
681 and cumulative spike train (CST) signals (bottom). Fascicle length data is presented as the amount

682 of shortening from rest to target torque (fascicle length during rest-fascicle length reached at
683 target torque). Note that fascicle shortening precedes the generation of torque during the ramp-
684 up phase of the contraction and then returns to baseline values after the torque signal returns
685 to zero. B) Common fluctuations from the three generated signals (torque, CST and fascicle
686 length) in the steady-torque part of the contraction can be seen on top of the figure. Cross-
687 correlation and lag (delay, ms) results between CST vs torque, CST vs fascicle length (fascicle) and
688 fascicle vs torque can be seen on the bottom of the figure.

689 **Figure 6.** Cross-correlation lag (delay) results during isometric contractions. Delays between
690 cumulative spike train (CST) vs torque, CST vs fascicle length (fascicle) and fascicle vs torque can
691 be seen for sustained isometric contractions at 0° and 30° of plantarflexion at 20% MVC (A) and
692 40% MVC (B). *, significant effect of joint angle ($p<0.05$).

693 **Figure 7.** Recruitment and de-recruitment thresholds in relation to torque and fascicle length. A
694 representative example of recruitment and de-recruitment threshold of a motor unit in relation
695 to torque and fascicle length can be seen on the left of the figure. The recruitment threshold for
696 this unit was higher than the de-recruitment threshold when calculated as %MVC torque (green
697 dashed line) but similar when calculated as fascicle shortening length (blue dashed line). Fascicle
698 length data is presented as the amount of shortening from rest to target torque (fascicle length
699 during rest-fascicle length reached at target torque). The same results can be appreciated by the
700 group of participants on the right of the figure as recruitment thresholds are consistently higher
701 than de-recruitment thresholds across target torques and angles when considered as %MVC
702 torque (upper right) but similar when calculated from fascicle length data (lower right). *,

703 significant effect of recruitment-de-recruitment ($p<0.05$). #, significant effect of joint angle

704 ($p<0.05$). Ψ, significant effect of torque ($p<0.05$).

705

706

707

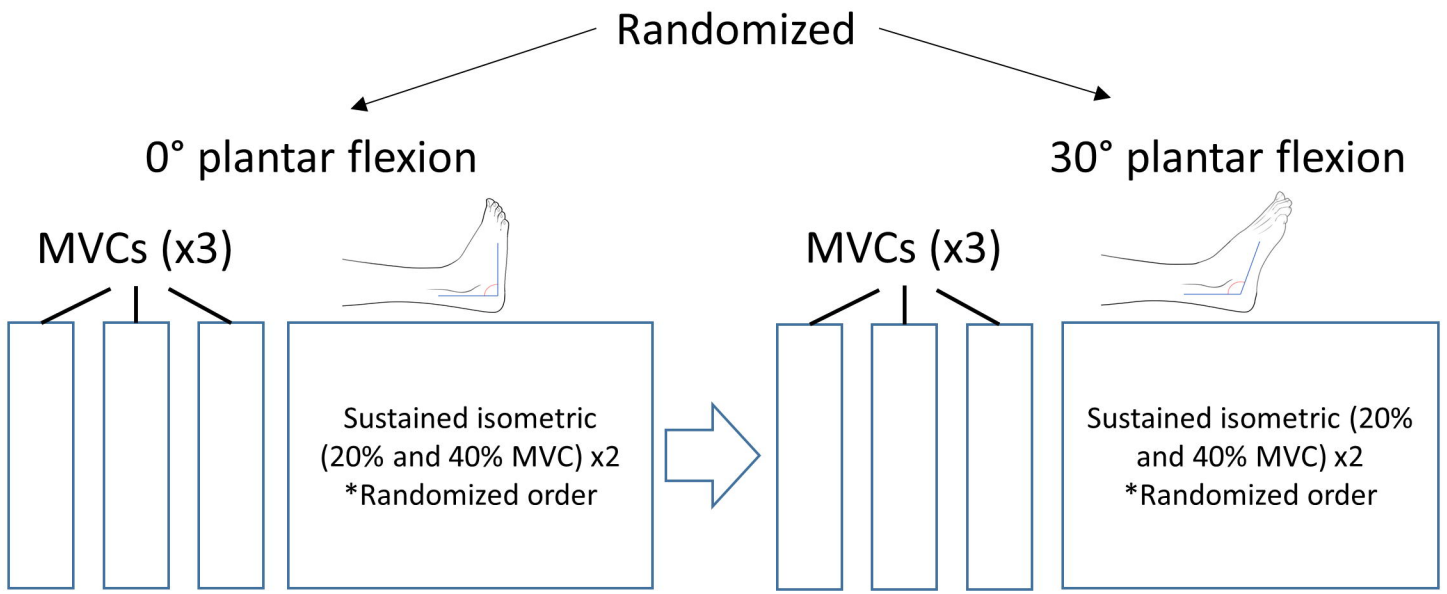
Randomized
0° plantar flexion
30° plantar flexion
MVCs (x3)
MVCs (x3)
Sustained isometric (20% and 40% MVC) x2 *Randomized order
Sustained isometric (20% and 40% MVC) x2 *Randomized order

A)

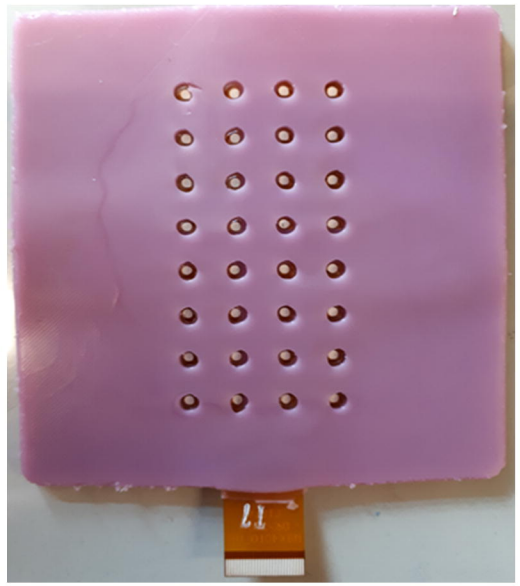

B)

Distal Proximal

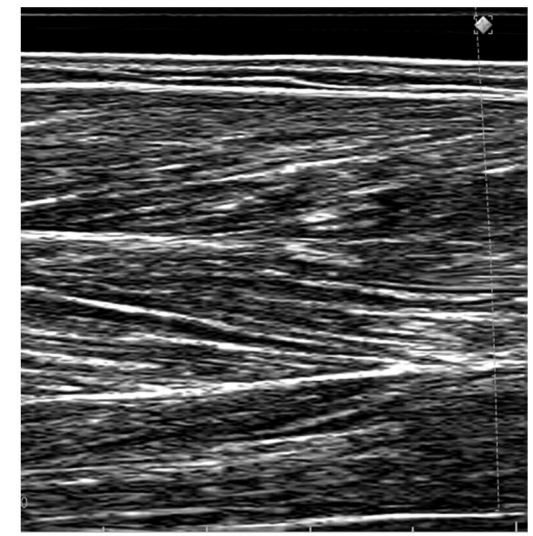

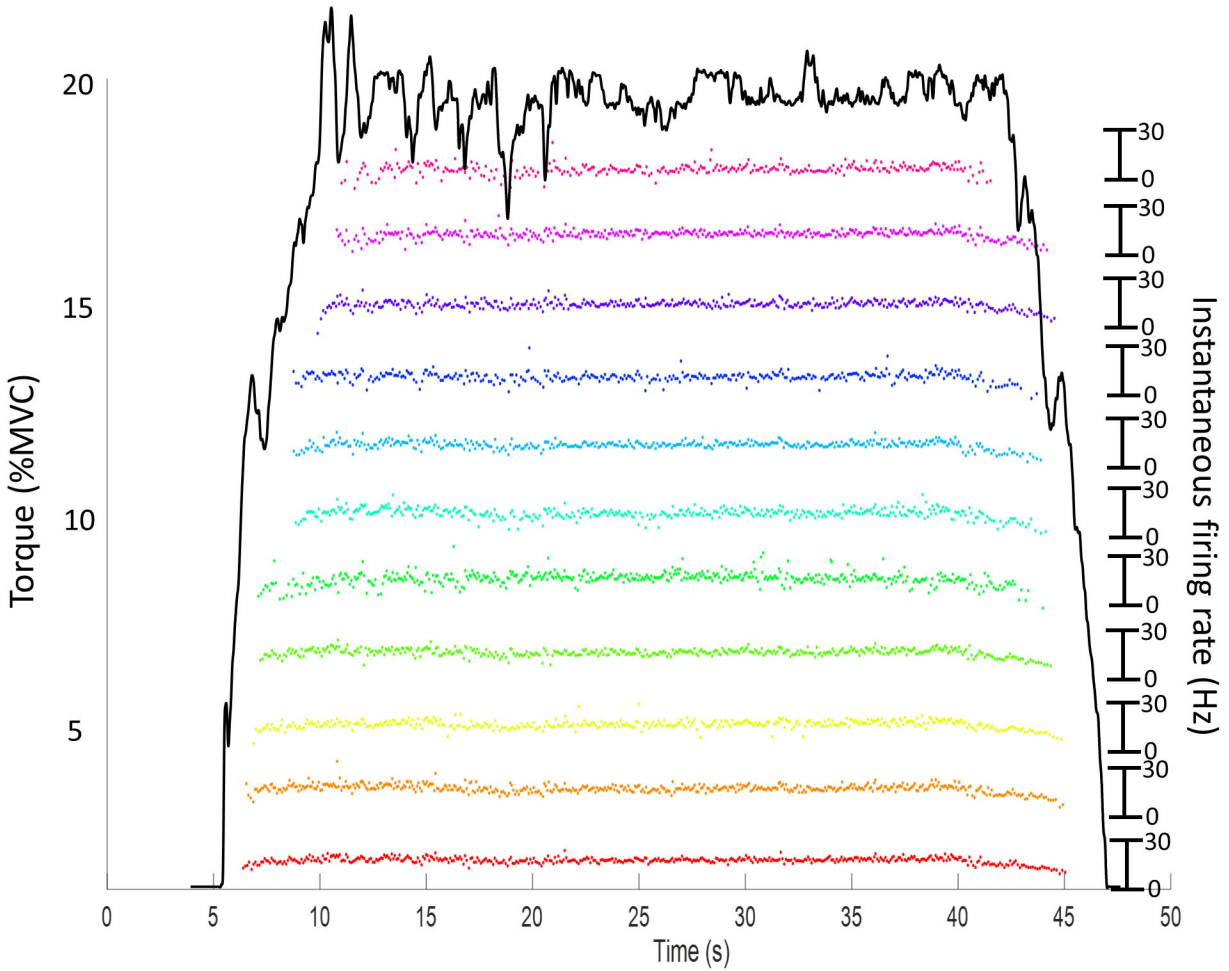
Torque (%MVC)
20
15
10
5
0
5
10
15
20
25
30
35
40
45
50
Time (s)
Instantaneous firing rate (Hz)
30
0

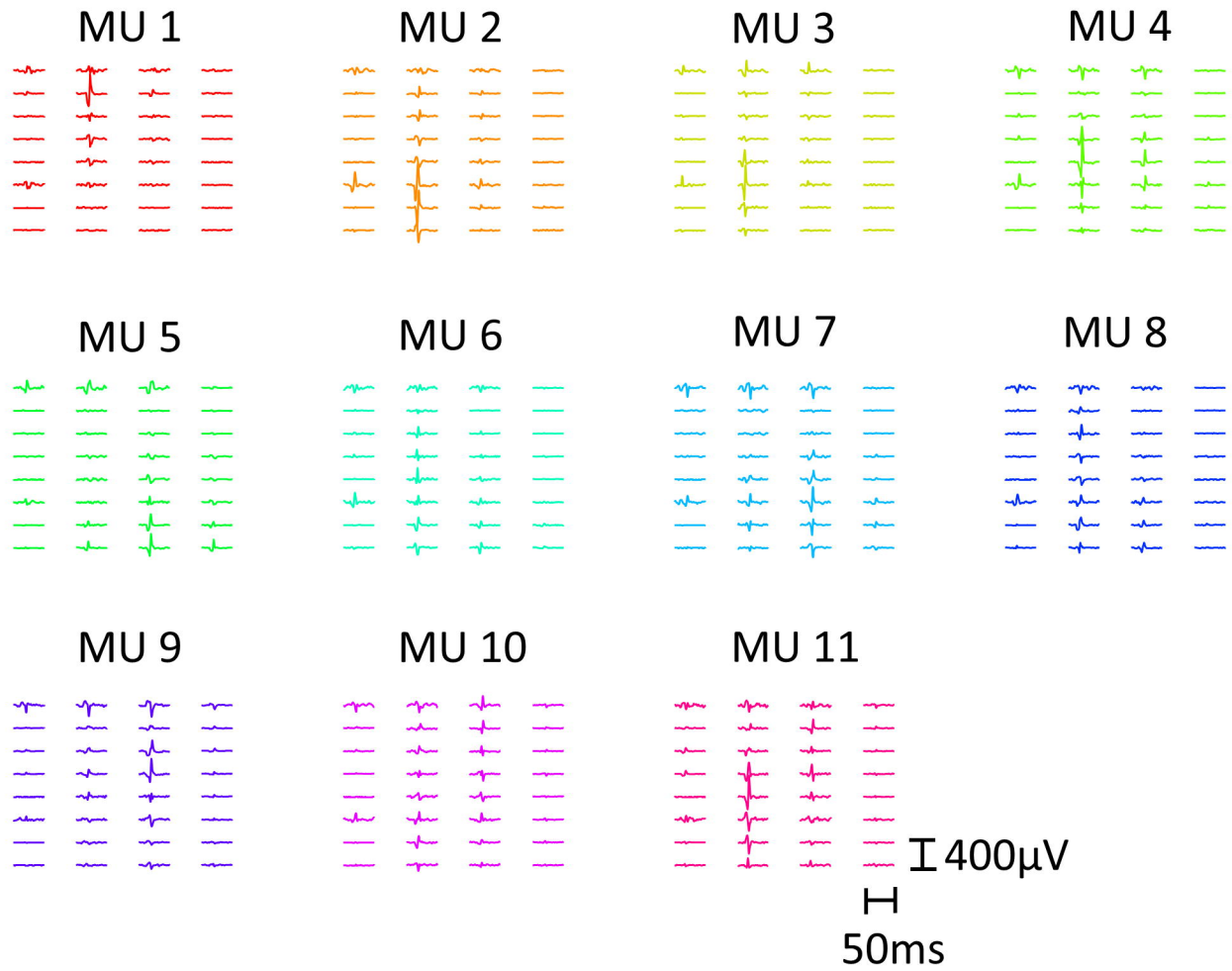
MU 1
MU 2
MU 3
MU 4
MU 5
MU 6
MU 7
MU 8
MU 9
MU 10
MU 11
400µV
50ms

Cross correlation = 0.91

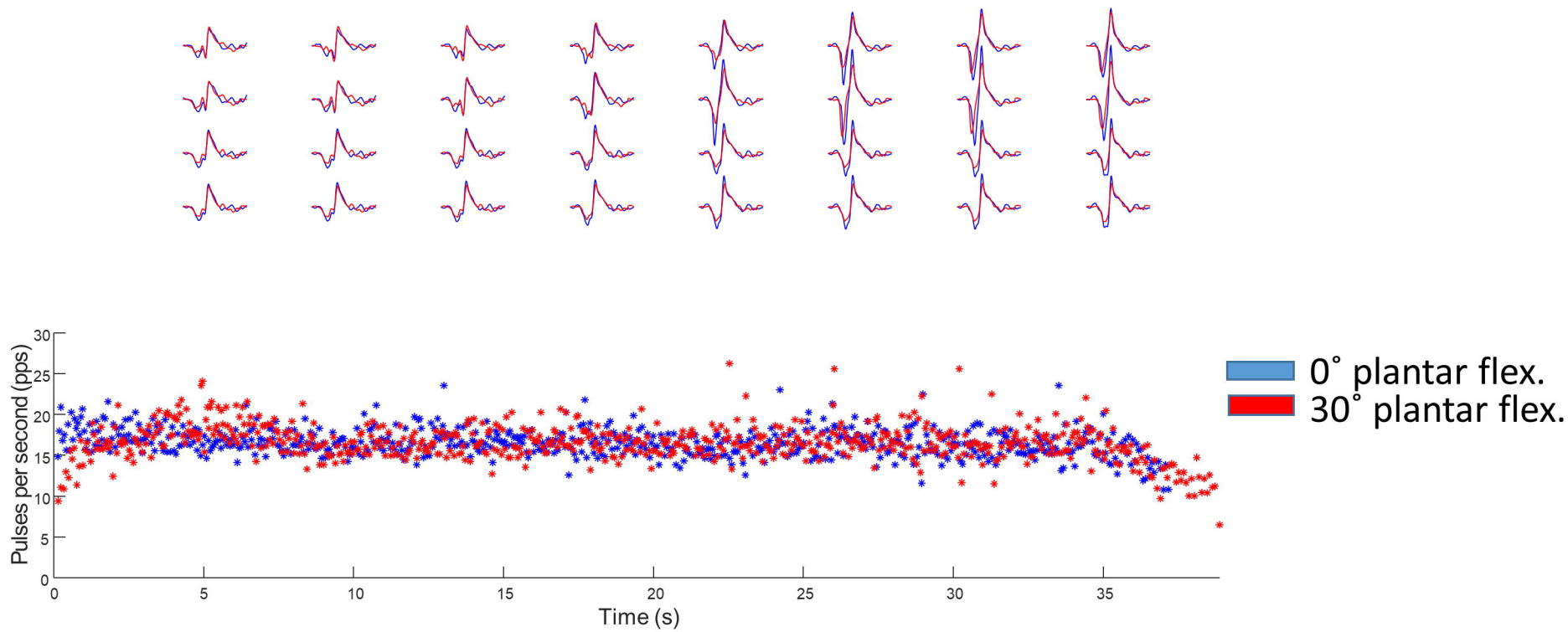

A)

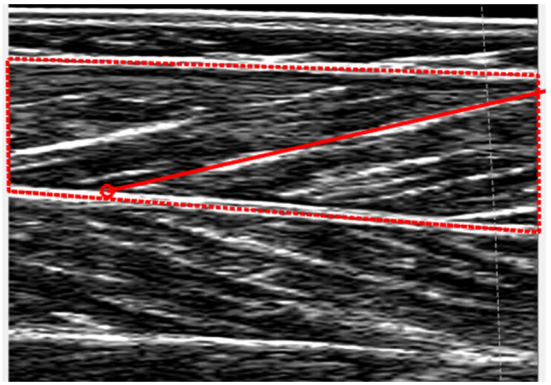

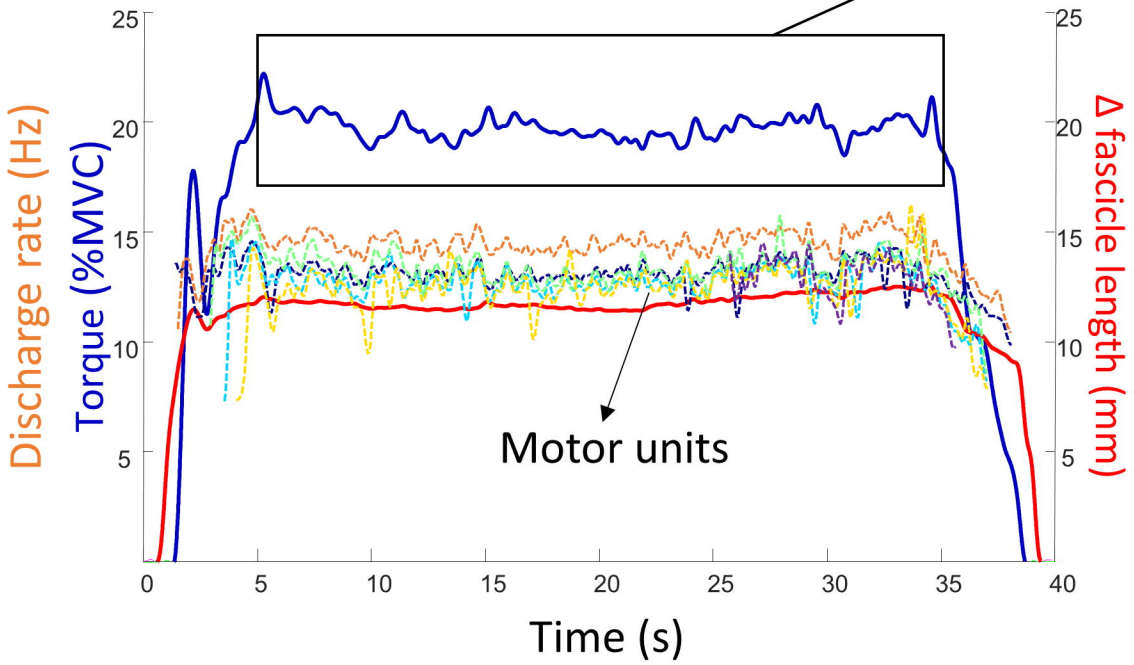

B)

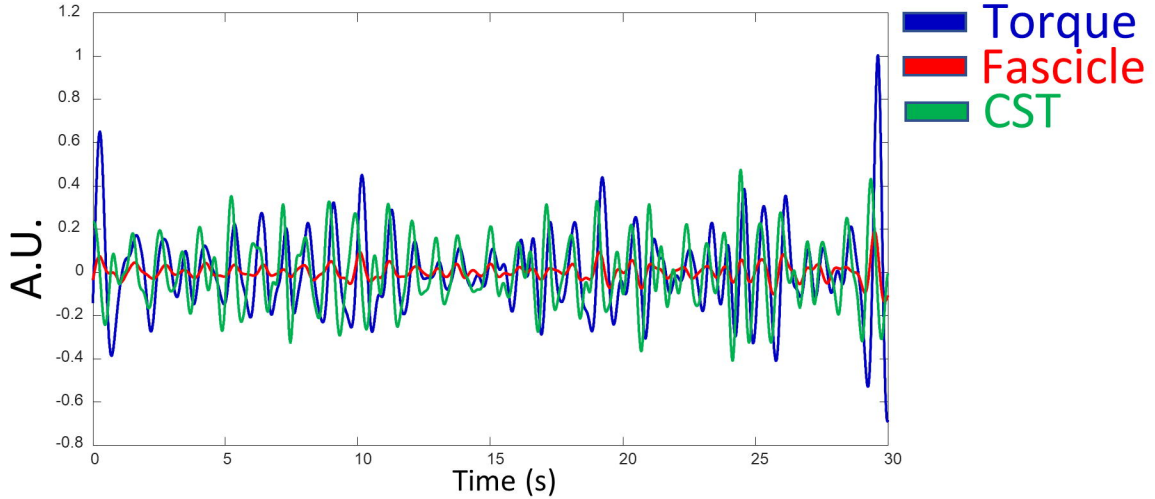

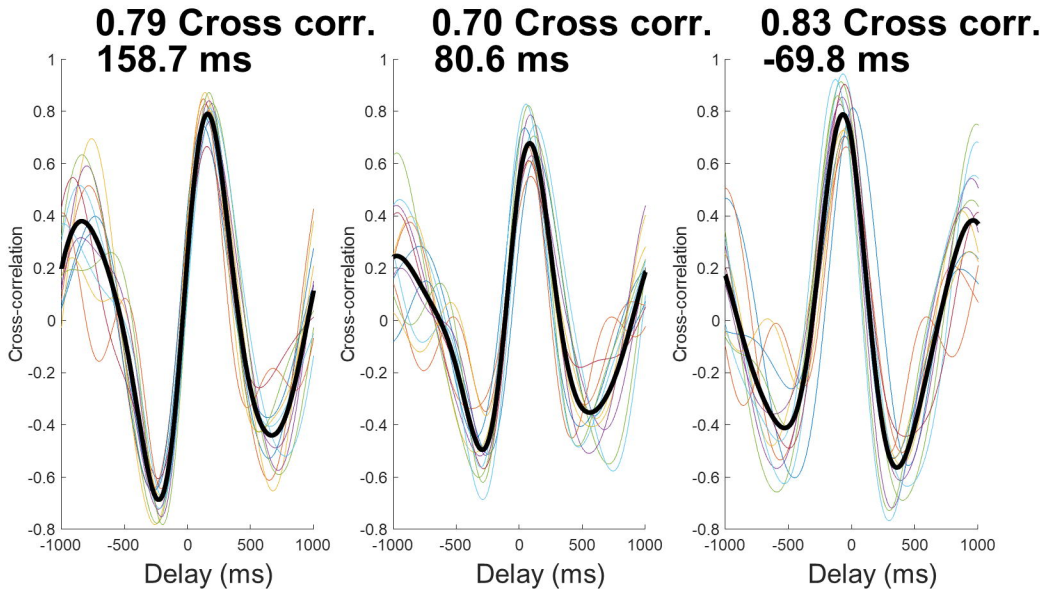

CST vs TORQUE CST vs FASCICLE TORQUE vs FASCICLE

A) Cross-correlation lag 20% MVC

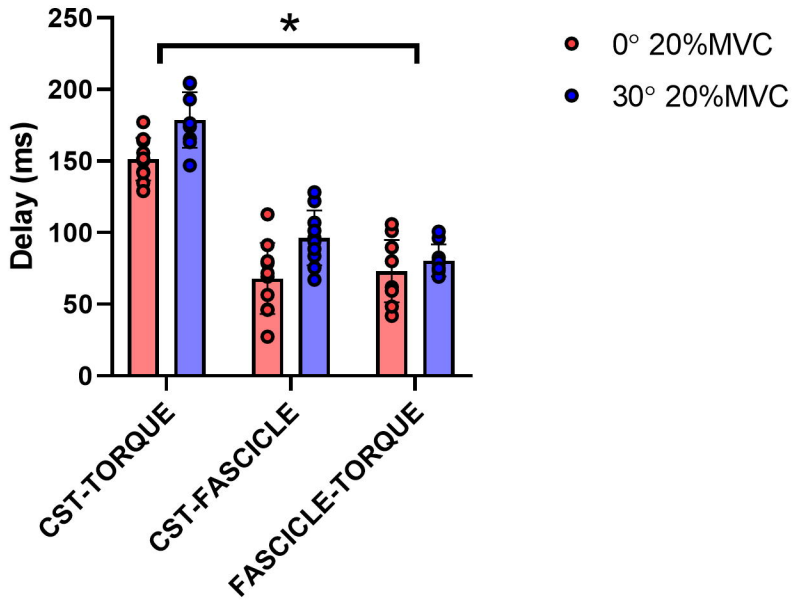

B) Cross-correlation lag 40% MVC

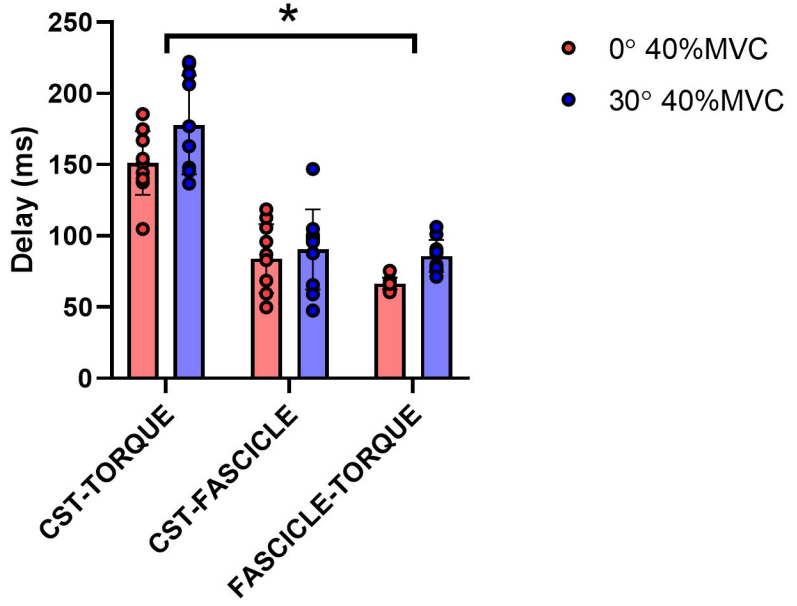

A)

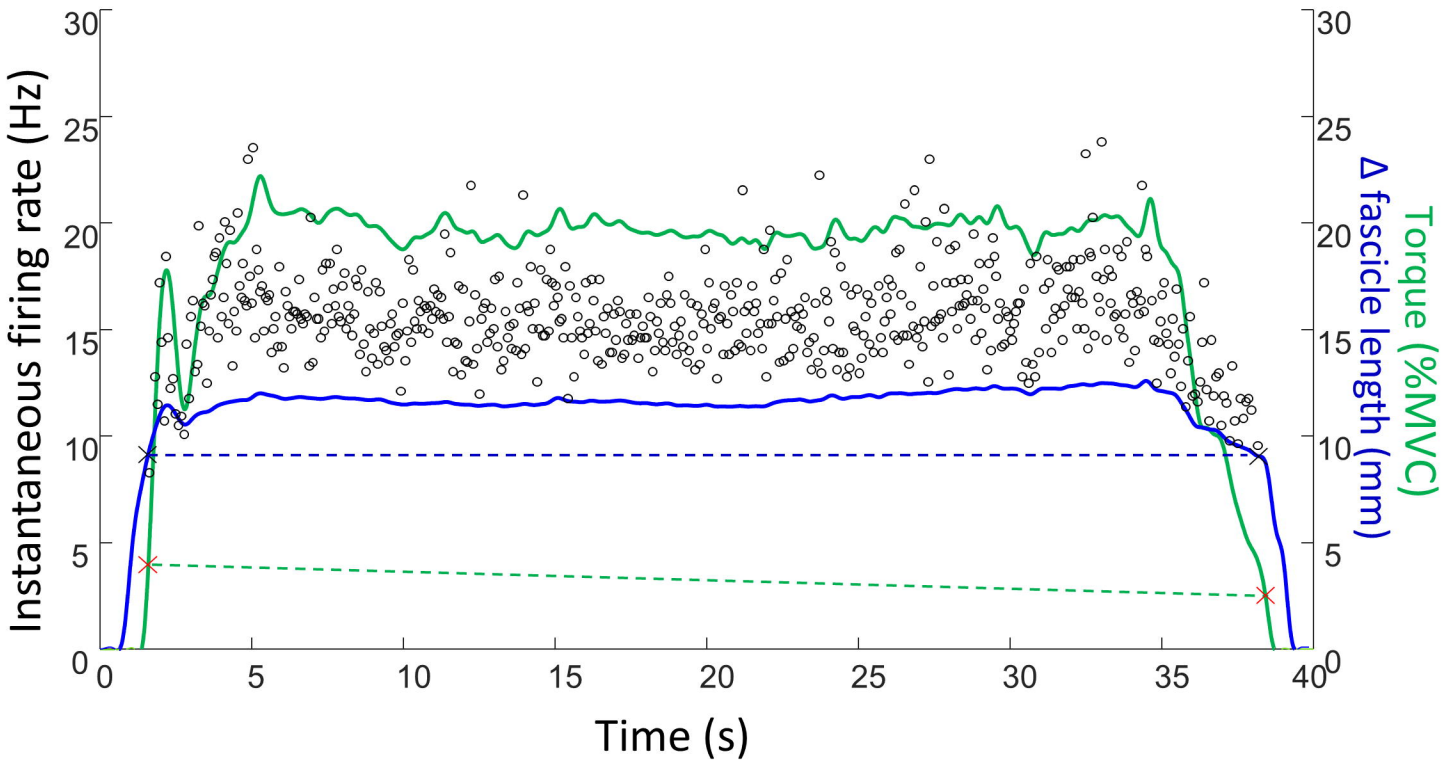
Instantaneous firing rate (Hz)
Torque (%MVC)
Δ fascicle length (mm)
Time (s)
0
5
10
15
20
25
30
35
40

B)

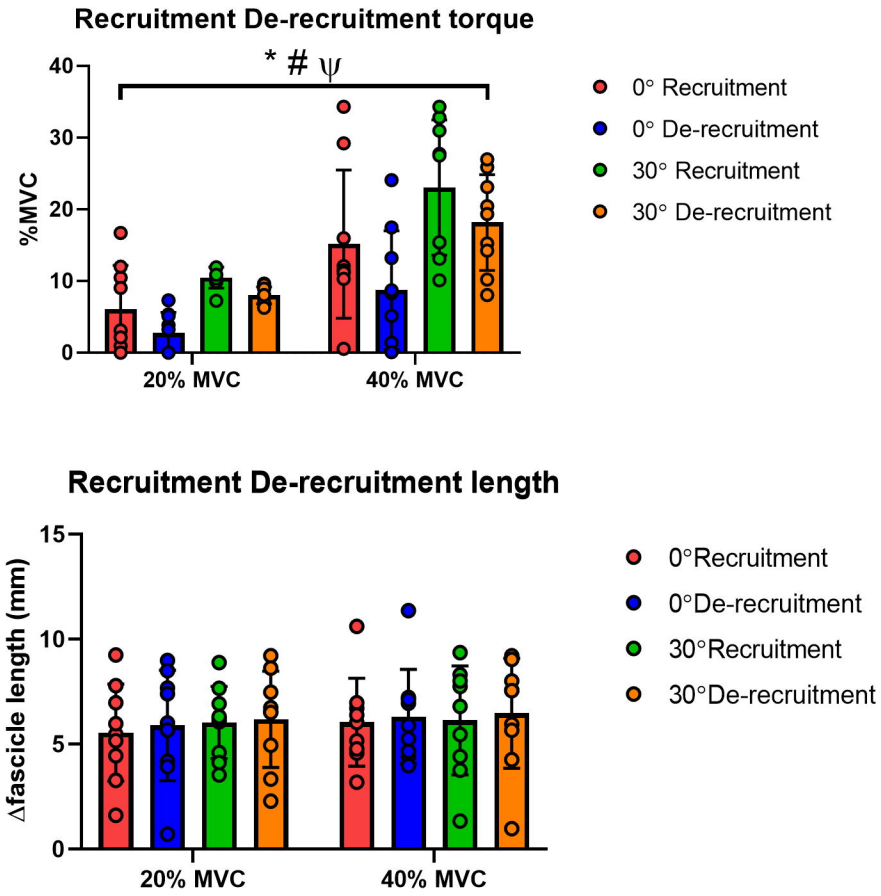
Recruitment De-recruitment torque
* # ψ
%MVC
20% MVC
40% MVC
0° Recruitment
0° De-recruitment
30° Recruitment
30° De-recruitment
Recruitment De-recruitment length
Δfascicle length (mm)
20% MVC
40% MVC
0°Recruitment
0°De-recruitment
30°Recruitment
30°De-recruitment